In situ generation, metabolism and immunomodulatory signaling actions of nitro-conjugated linoleic acid in a murine model of inflammation

Luis Villacorta[a,*], Lucia Minarrieta[b,c], Sonia R. Salvatore[d], Nicholas K. Khoo[d], Oren Rom[a], Zhen Gao[a], Rebecca C. Berman[a], Soma Jobbagy[d], Lihua Li[d], Steven R. Woodcock[d], Y. Eugene Chen[e], Bruce A. Freeman[d], Ana M. Ferreira[b], Francisco J. Schopfer[d], Dario A. Vitturi[d,**]

[a] Department of Internal Medicine, Frankel Cardiovascular Center, University of Michigan Medical Center, Ann Arbor, MI, USA
[b] Cátedra de Inmunología, Facultad de Química y Ciencias, Universidad de la República, Montevideo, Uruguay
[c] Institute of Infection Immunology, TWINCORE, Hannover, Germany
[d] Department of Pharmacology and Chemical Biology, University of Pittsburgh, Pittsburgh, PA, USA
[e] Department of Cardiac Surgery, Frankel Cardiovascular Center, University of Michigan Medical Center, Ann Arbor, MI, USA

ARTICLE INFO

ABSTRACT

Conjugated linoleic acid (CLA) is a prime substrate for intra-gastric nitration giving rise to the formation of nitro-conjugated linoleic acid (NO_2-CLA). Herein, NO_2-CLA generation is demonstrated within the context of acute inflammatory responses both in vitro and in vivo. Macrophage activation resulted in dose- and time-dependent CLA nitration and also in the production of secondary electrophilic and non-electrophilic derivatives. Both exogenous NO_2-CLA as well as that generated in situ, attenuated NF-κB-dependent gene expression, decreased pro-inflammatory cytokine production and up-regulated Nrf2-regulated proteins. Importantly, both CLA nitration and the corresponding downstream anti-inflammatory actions of NO_2-CLA were recapitulated in a mouse peritonitis model where NO_2-CLA administration decreased pro-inflammatory cytokines and inhibited leukocyte recruitment. Taken together, our results demonstrate that the formation of NO_2-CLA has the potential to function as an adaptive response capable of not only modulating inflammation amplitude but also protecting neighboring tissues via the expression of Nrf2-dependent genes.

1. Introduction

Inflammatory responses are central to survival in the face of sterile and infectious insults. However, equally important as being able to mount an effective response is the ability to terminate this process when the threat has been removed [1]. Indeed, chronic inflammation is a driving force behind metabolic syndrome development [2], atherogenesis [3], occurrence of acute cardiovascular events [4,5] and progression to heart failure [6]. As a result, the immune system must be endowed with mechanisms that allow it to sensitively respond to a changing inflammatory environment and achieve self-limitation [1]. Inflammation is initiated by a complex series of events, that include the activation of toll-like receptors (TLR) in resident macrophages, dendritic cells and non-immune cells by pathogen- and damage-associated molecular patterns (PAMPs and DAMPs, respectively). This activation leads in turn to microvasculature changes, which mediate the recruitment of neutrophils and monocytes into the inflamed tissues [7]. At these sites, leukocyte activation results in increased nitric oxide ('NO) and superoxide generation by iNOS and NADPH-oxidases respectively, leading to peroxynitrite and ultimately 'NO$_2$ formation [8]. In addition, myeloperoxidase (MPO) released by neutrophil degranulation in the presence of hydrogen peroxide and nitrite also contributes to 'NO$_2$ formation [9]. The generation of reactive nitrogen oxides is an essential component of the early response to invading pathogens [8,10]. Herein

we show that in addition to their well-characterized microbicidal actions, reactive nitrogen oxides fine-tune the inflammatory response via the formation and signaling actions of NO_2-CLA.

Nitrated fatty acids (NO_2-FA) are generated upon ˙NO_2 addition to double bonds in unsaturated fatty acids [11]. The resulting nitroalkene moiety confers NO_2-FAs with electrophilic reactivity thus allowing them to reversibly interact with nucleophilic cysteines both in proteins and in low molecular weight compounds [12,13]. This covalent reactivity is essential for their numerous biological actions, including Nrf2 activation, partial PPARγ agonism, heat shock response induction and TLR4/NF-κB/STAT1 inhibition [14–16]. Administration of the prototypical NO_2-FA, nitro-oleic acid (NO_2-OA) is associated with improved outcomes in a wide range of animal models of disease, which has propelled the pharmacological development of NO_2-FA as drug candidates for clinical use (http://www.complexarx.com/).

CLA has recently been identified as a prominent substrate for NO_2-CLA formation *in vivo* [17]. CLA is present in dairy and meat-derived products and becomes nitrated upon reaction with nitrite derived from saliva and diets rich in leafy vegetables in the acidic conditions of the stomach, [18–21]. As a result, NO_2-CLA is detected in varying amounts in the plasma (1–3 nM) and urine (0.5–43 pmol/mg creatinine) of healthy human subjects, and its levels can be further modulated by oral supplementation with CLA in combination with either nitrite or nitrate [19,22]. Interestingly, although consumption of CLA alone has been sporadically associated with anti-inflammatory effects both in animal models and human studies, the clinical significance of these findings remains poorly defined [21,23–25].

NO_2-CLA levels under healthy conditions are most likely determined by the diet [19]. However, the generation of ˙NO_2 during inflammatory responses has the potential to be a prominent pathway for *in situ* NO_2-CLA formation. Using high resolution mass spectrometry and stable isotope dilution quantitation techniques, we demonstrate that inflammatory macrophages mediate CLA nitration in a dose- and time-dependent manner. This reaction is dependent on iNOS activity and leads to the formation of two positional NO_2-CLA isomers which are further metabolized by macrophages. Both isomers activated Nrf2 signaling and inhibited the transcription of NF-κB-dependent genes, resulting in the suppression of pro-inflammatory cytokine production and in the expression of cytoprotective phase 2 proteins. Notably, the anti-inflammatory effects of NO_2-CLA were corroborated *in vivo* using a mouse model of zymosan-A induced peritonitis that promotes *in situ* CLA nitration. Taken together, our results support that NO_2-CLA formation is an adaptive response capable of down-regulating inflammation and protecting neighboring tissues against the deleterious effects of reactive oxygen and nitrogen species.

2. Results

2.1. LPS/IFN-γ activated macrophages mediate CLA nitration and subsequent NO_2-CLA metabolism

RAW264.7 macrophages were activated in the presence of CLA (50 μM) and the formation of nitrated derivatives was assessed in the media 24 h later. Fig. 1 shows the formation of both NO_2-CLA (Fig. 1A) and its two-electron reduction product dihydro-NO_2-CLA (Fig. 1B). A set of two closely-eluting isobaric peaks were detected for both NO_2-CLA and dihydro-NO_2-CLA. In the case of NO_2-CLA, MS^2 fragmentation analysis and accurate mass determinations identified these species as the positional 12- and 9-NO_2-CLA isomers (peaks 1 and 2 respectively, Fig. S1A). Unlike nitroalkene-containing fatty acids, collision induced dissociation of nitroalkane dihydro-derivatives does not result in structurally-informative fragment ions beyond the typical neutral losses of H_2O, CO_2 and HNO_2 [26]. Therefore, the identity of the two dihydro-NO_2-CLA peaks was established by a combination of high resolution accurate mass determinations (Fig. S1B) and co-elution with a synthetic dihydro-9-$^{15}NO_2$-CLA standard (Fig. 1B). As expected, the formation of NO_2-CLA and dihydro-NO_2-CLA was dependent on CLA concentration and time after activation for both RAW264.7 and bone marrow-derived macrophages (BMDM) (Fig. 1C-E). Interestingly, CLA nitration was only observed in the presence of the classic M1 inducers LPS/IFN-γ, with no NO_2-CLA formation obtained by either non-activated or M2-polarized macrophages (Fig. 1E). These results suggested an important role for the NF-κB-regulated gene iNOS, as this protein in the main source of ˙NO production under inflammatory conditions. Consistent with this hypothesis, NO_2-CLA formation was completely abrogated by both the iNOS-specific inhibitor 1400 W or the use of iNOS$^{-/-}$ derived BMDM (Fig. 1F).

In addition to nitroalkene reduction to the corresponding dihydro-derivative, NO_2-FA also undergo β-oxidation giving rise to dinor, tetranor and hexanor metabolites [27]. Incubation of RAW264.7 cells with synthetic NO_2-CLA resulted in the generation of two series of metabolites separated by 28 amu corresponding to successive losses of C_2H_4 from both the parent compound and the dihydro-NO_2-CLA derivative (Fig. 2A, top). This pattern was fully recapitulated when activated RAW264.7 cells are treated with CLA (Fig. 2A, middle), indicating that macrophages can modulate NO_2-CLA levels by mediating both its formation and catabolism. Previous work indicates that only nitroalkene-containing NO_2-FA are electrophilic [22,28]. To test this, macrophage media containing endogenously generated NO_2-CLA was incubated with excess β-mercaptoethanol (BME) nucleophile before lipid extraction. As expected, BME treatment resulted in selective consumption of nitroalkene-containing NO_2-CLA metabolites whilst having no effect on the levels of non-electrophilic dihydro-NO_2-CLA derivatives (Fig. 2A, bottom). In line with the results obtained with NO_2-CLA formation, the levels of both nitroalkene-containing and dihydro β-oxidation metabolites increased as a function of incubation time and CLA concentration (Fig. 2B-E).

2.2. Positional isomers of NO_2-CLA have different catabolic rates

Nitrogen dioxide adds to carbons C9 and C12 in the diene moiety of 9,11-CLA forming 9-NO_2-CLA and 12-NO_2-CLA with similar efficiency [17,29]. However, isomer-specific analysis of NO_2-CLA formation by activated RAW264.7 cells revealed preferential accumulation of the 9-NO_2-CLA derivative (Fig. 3A). This coincided with a more predominant formation of the reduced metabolite dihydro-12-NO_2-CLA, suggesting that 12-NO_2-CLA is metabolized more readily than the 9-NO_2-CLA isomer (Fig. 3B). To test this concept, RAW264.7 cells were independently treated with synthetic 9- and 12-NO_2-CLA and catabolism was monitored. Consistent with the hypothesis, 12-NO_2-CLA was consumed at a significantly higher rate and resulted in a more prominent formation of the corresponding dihydro-12-NO_2-CLA derivative than 9-NO_2-CLA (Fig. 3C-D).

2.3. NO_2-CLA inhibits pro-inflammatory signaling and promotes expression of Nrf2-dependent genes

To test the role of NO_2-CLA in modulating pro-inflammatory signaling, RAW264.7 cells were activated with LPS/IFN-γ in the presence of increasing does of either 9-NO_2-CLA or 12-NO_2-CLA. The more efficient reduction of 12-NO_2-CLA versus 9-NO_2-CLA (see Fig. 3) suggested that the latter might be a more potent signaling mediator. However, Fig. 4A demonstrates that both isomers inhibited the expression of the NF-κB target protein iNOS with comparable potency. Consistent with this observation, NO_2-CLA co-treatment also dose-dependently inhibited the secretion of the pro-inflammatory cytokines IL-6 and MCP-1 by RAW264.7 cells (Fig. 4B-C) and directly antagonized the expression of NF-κB-dependent genes as demonstrated using a luciferase-based reporter construct (Fig. S2A). Finally, these results were recapitulated in BMDM, where NO_2-CLA potently inhibited LPS/IFN-γ induced iNOS and IL-6 expression (Fig. 4D-E). Interestingly, the observation that macrophage activation with LPS/IFN-γ leads to iNOS-dependent CLA
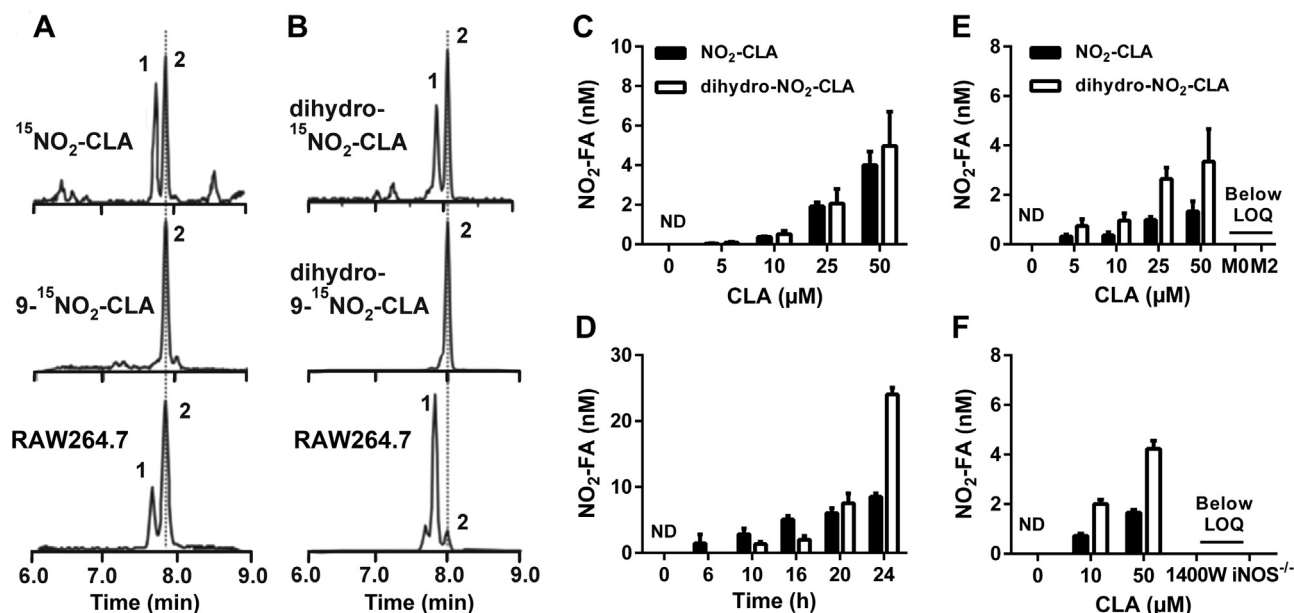
Fig. 1. LPS/IFN-γ activated macrophages generate NO₂-CLA. RAW264.7 were activated in the presence of 50 μM CLA for 24 h and NO₂-FA formation measured in media. A) MRM analysis for synthetic mixed ^{15}NO₂-CLA (top), synthetic 9-^{15}NO₂-CLA (middle) and RAW264.7-generated NO₂-CLA (bottom). B) Detection of dihydro-NO₂-CLA by MRM analysis. Panels show mixed dihydro-^{15}NO₂-CLA (top), dihydro-9-^{15}NO₂-CLA (middle) and RAW264.7-derived dihydro-NO₂-CLA (bottom). Peaks 1 and 2 indicate the corresponding 12-NO₂ and 9-NO₂ positional isomers. C-D) Dose- and time-dependence of NO₂-FA formation by activated RAW264.7 cells. Data are represented as mean ± SEM (n = 3–6). E) Dose-response for NO₂-FA formation by M1, M2 and M0 polarized BMDM. F) NO₂-FA formation in wild-type (WT) BMDM, WT in the presence of the iNOS inhibitor 1400 W (100 μM) or in iNOS$^{-/-}$ BMDM. Dose responses were established at 20 h and time courses were generated using 50 μM CLA. Data are represented as mean ± SEM (n = 4). ND: Not detected. LOQ: Limit of quantification.
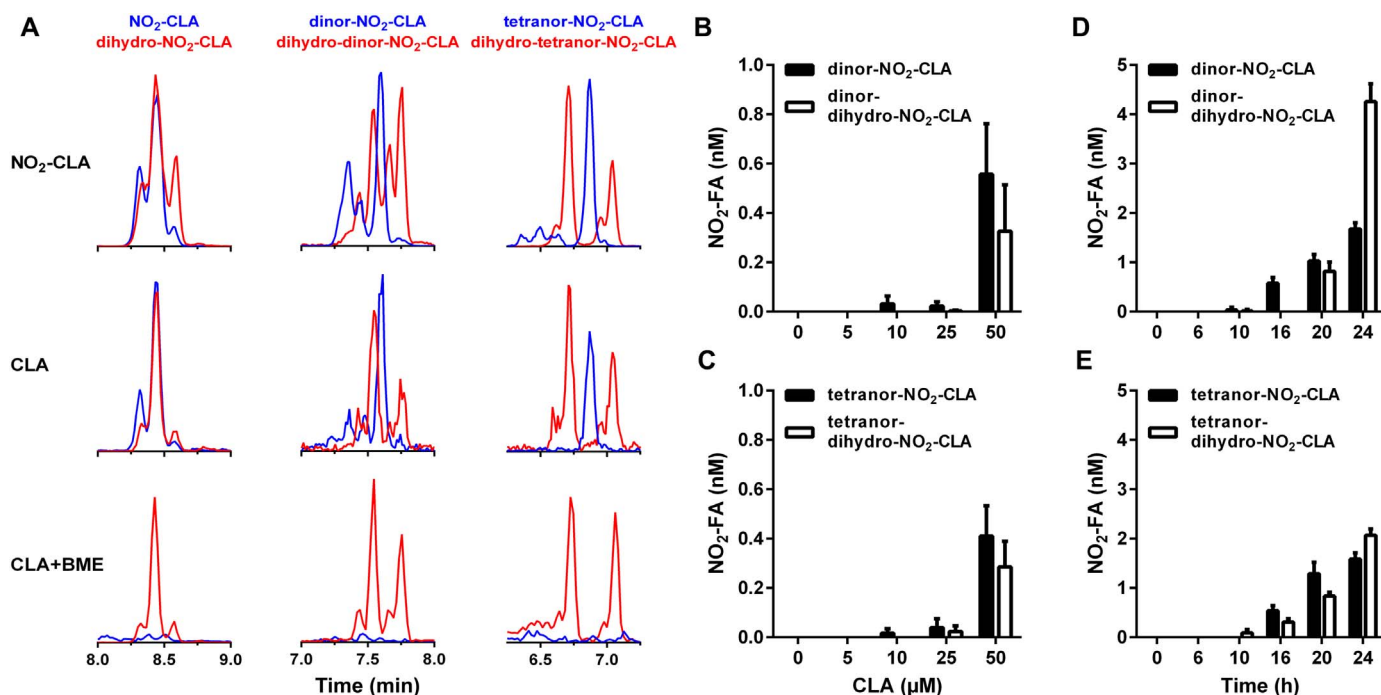

Fig. 2. In situ generated NO₂-CLA is metabolized by macrophages. A) Representative LC-MS/MS traces obtained after 24 h incubation of LPS/IFN-γ activated RAW264 cells with synthetic NO₂-CLA (5 μM, top) or in situ formed NO₂-CLA (from 50 μM CLA, middle). Blue traces correspond to unsaturated nitroalkene species and red traces correspond to saturated dihydro metabolites. Unsaturated metabolites retain electrophilic reactivity as indicated by their complete consumption upon incubation with 500 mM BME for 2 h before extraction as opposed to dihydro-derivatives which are not affected by BME treatment (bottom). Dose and time-dependence for the generation of one- (B, D) and two-round (C, E) β-oxidation metabolites of NO₂-CLA and dihydro-NO₂-CLA derivatives by LPS/IFN-γ activated RAW264.7 cells. Data are means ± SEM (n = 3–6).

nitration (Fig. 1) and that synthetic NO₂-CLA is in turn capable of down-regulating NF-κB dependent genes, hinted at the existence of a potential feedback mechanism. In this regard, CLA dose-dependently inhibited LPS/IFN-γ mediated IL-6 and iNOS expression but this effect was lost when iNOS activity was abrogated by either genetic ablation (Fig. 4F) or pharmacological inhibition (Fig. 4G).

In addition to their antagonistic effects on pro-inflammatory signaling, electrophilic NO₂-FAs also activate transcription of Nrf2-dependent genes via covalent modification of cysteines 273 and 288 in Keap1 [30–32]. Consistent with this notion, addition of both 9- and 12-NO₂-CLA to RAW264.7 cells led to concomitant increases in HO-1 and NQO-1 expression (Fig. 5A), with similar results obtained using BMDM

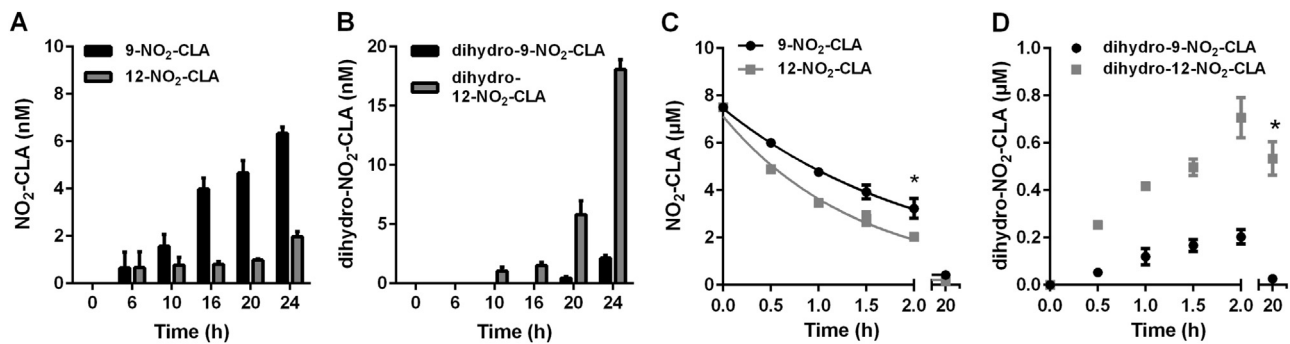**Fig. 3. Differential accumulation and metabolism of NO_2-CLA positional isomers.** Time-dependent generation of 9- and 12-NO_2-CLA (A) and their corresponding reduction metabolites (B) by LPS/IFNγ activated RAW264.7 cells. Data are means ± SD (n = 3–6). Synthetic 12-NO_2-CLA is more efficiently metabolized by RAW264.7 cells (C) leading to a more prominent accumulation of dihydro-12-NO_2-CLA (D). Data are means ± SD (n = 3) * p < 0.05 as determined by two-way ANOVA.

(Fig. 5B-D). In this regard, whereas Nrf2-independent mechanisms have been shown to contribute to the regulation of HO-1 expression [33], the increase in NQO-1 levels strongly suggests Nrf2 activation. These results were confirmed using an Nrf2/ARE-dependent luciferase reporter system, where either mixed or pure NO_2-CLA isomers resulted in dose-dependent increases in luciferase activity (Fig S2B).

2.4. In vivo inflammatory NO_2-CLA formation

To define whether CLA nitration also occurs in an *in vivo* inflammatory setting, C57BL/6 J mice were injected with zymosan-A particles from *S. cerevisiae* followed by CLA (2.5 mg). The time of CLA administration was set at 12 h post zymosan-A dosing to coincide with the peak of leukocyte infiltration [34]. Peritoneal lavages were obtained 1–6 h after CLA injection and NO_2-CLA formation was assessed. Mass spectrometric specific detection of 9- and 12-NO_2-CLA indicates

that both positional isomers are formed in the peritoneal cavity during the inflammatory response (Fig. 6A). Total NO_2-CLA formation is highest during the first hour post CLA administration (21.25 ± 9.53 nM) and then levels decrease progressively throughout the observation period (Fig. 6B). No NO_2-CLA was detected in the absence of CLA supplementation.

2.5. NO_2-CLA regulates acute inflammatory responses

The effects of NO_2-CLA on the inflammatory response were assessed *in vivo* using the same zymosan-A induced self-resolving inflammation model. To better understand the effects of NO_2-CLA on the entire course of the inflammatory response, mice were allocated to receive CLA (2.5 mg/mouse) or NO_2-CLA (2.5 mg/kg) at the time of zymosan-A injection. Under these co-administration conditions, CLA supplementation resulted in low levels of nitration (1.23 ± 0.69 nM NO_2-CLA
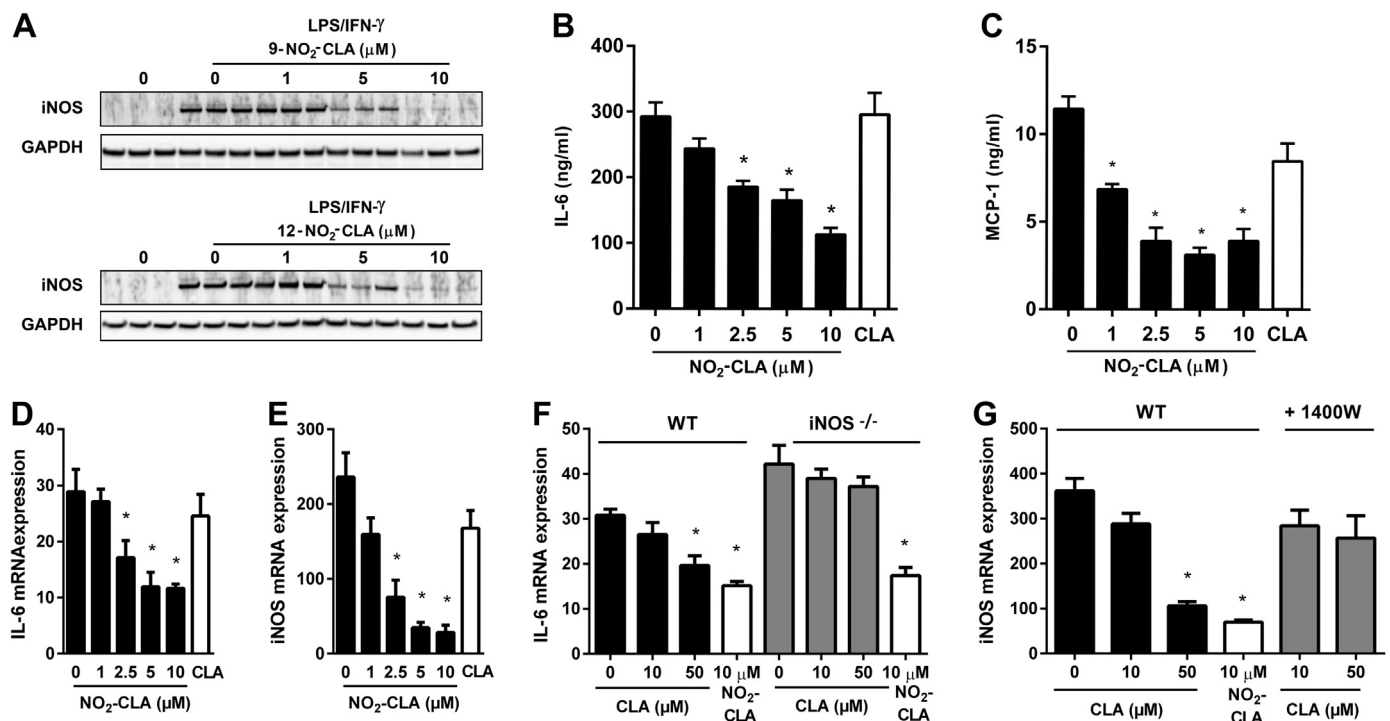
Fig. 4. NO_2-CLA inhibits NF-κB signaling. A) Dose-dependent inhibition of iNOS expression in LPS/IFN-γ activated RAW264.7 cells by synthetic 9- and 12-NO_2-CLA. B-C) Inhibition of IL-6 and MCP-1 secretion by activated RAW264.7 cells after 24 h co-treatment with CLA (10 μM) or the indicated NO_2-CLA doses. Data are shown as means ± SEM. * p < 0.05 vs. no NO_2-CLA controls as determined by one-way ANOVA and Dunnett's multiple comparisons test (n = 3–4). D-E) Dose-dependent NO_2-CLA inhibition of IL-6 and iNOS gene expression in LPS/IFN-γ activated BMDM. Data are means ± SEM. * p < 0.05 vs. no NO_2-CLA controls as determined by one-way ANOVA and Dunnett's multiple comparisons test (n = 4). F-G) CLA inhibition of IL-6 and iNOS expression in LPS/IFN-γ activated BMDM is dependent on iNOS activity as demonstrated by the use of iNOS$^{-/-}$ BMDM and the iNOS inhibitor 1400 W (100 μM). Data is presented as mean ± SEM. * p < 0.05 as determined by one-way ANOVA and Dunnett's multiple comparisons test vs. corresponding no CLA controls (n = 4).
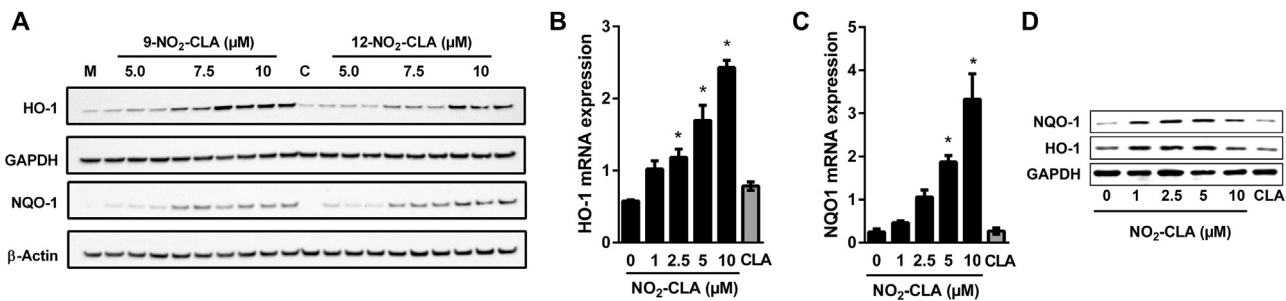
Fig. 5. NO$_2$-CLA activates Nrf2 signaling. A) Dose-dependent induction of HO-1 and NQO-1 expression by 9- and 12-NO$_2$-CLA in RAW264.7 cells. M: Methanol vehicle control. C: CLA (10 µM). B-C) NO$_2$-CLA induces HO-1 and NQO-1 expression in LPS/IFN-γ activated BMDM. Data are means ± SEM. * p < 0.05 as determined by one-way ANOVA and Dunnett's multiple comparisons test vs. no NO$_2$-CLA controls (n = 4). CLA treatment (10 µM) had no effect on mRNA levels. D) HO-1 and NQO-1 protein induction by NO$_2$-CLA or CLA (10 µM) treatment in in LPS/IFN-γ activated BMDM.

at 12 h, n = 6) while synthetic NO$_2$-CLA injection yielded 41.88 ± 29.88 nM (12 h, n = 6). Peritoneal exudates were collected to monitor temporal changes in the leukocyte composition by flow cytometry. Immune cell subsets within the peritoneal cavity were characterized as follows: neutrophils (PMN) (CD11b$^+$, CD19$^-$, F4/80$^-$ Ly6-G$^+$), monocytes (CD11b$^+$, CD19$^-$, F4/80^{int}, Ly-6G$^-$, Ly-6C$^+$), macrophages (CD11b$^+$, CD19$^-$, F4/80^{high}, Ly-6G$^-$), (Fig. S3). Following zymosan-A challenge, PMN infiltrate the peritoneal cavity during the onset phase of acute inflammation reaching a maximum at ~12 h of (Ψ_{max} ~11.6 × 10^6), followed by a decline at 24 h (~4.94 × 10^6) characteristic of the resolution phase [34] (Fig. 7). Differential flow cytometry analysis confirmed that the majority of extravasated leukocytes at 12 h were Ly-6G^{high} PMN, which represented ~80% of the total population (Fig. 7A) in both vehicle and CLA-treated groups. Administration of NO$_2$-CLA however, significantly limited PMN transmigration into the peritoneum as indicated by both decreased population abundance and reduced cell numbers (Fig. 7A and B). In line with this observation, assessment of pro-inflammatory cytokines in the peritoneal exudates at 12 h revealed a significant reduction in MCP-1 and IL-6 levels by NO$_2$-CLA treatment (Fig. 7C-D) consistent with in vitro anti-inflammatory effects (Fig. 4). Thus progression towards the resolution stage is not altered resulting in a further limited population of extravasated PMN by NO$_2$-CLA at 24 h (Fig. 7A). Interestingly, CLA co-administration with zymosan-A induced a modest reduction in total PMN numbers at 12 h but had no statistically significant effect on cytokine levels (Fig. 7B). Finally, as expected, the resident F4/80^{high} Ly-6G$^-$ macrophage population dropped after 12 h zymosan-A administration,

being replaced by F4/80^{int} Ly-6C$^+$ inflammatory monocytes (Fig. 7A and Fig. S4) [34]. Monocyte infiltration was not affected by either NO$_2$-CLA or CLA treatment (Fig. S4).

3. Discussion

The present report provides an integrated picture for the formation, metabolism, and immunomodulatory effects of NO$_2$-CLA as a potential adaptive signaling mediator under inflammatory conditions (Scheme 1). Unlike oleic and bis-allylic linoleic acid-derived NO$_2$-FAs, NO$_2$-CLA formation occurs at significant rates under conditions readily found in vivo [17]. The conjugation of the double bond system activates the external diene carbons in CLA towards reaction with $^\bullet$NO$_2$, thus promoting facile NO$_2$-CLA generation both secondary to nitrite acidification in the stomach and as a consequence of $^\bullet$NO autoxidation and symmetric dinitrogen trioxide (N$_2$O$_3$) formation in tissues [17,35]. NO$_2$-CLA is endogenously present in human plasma and urine under healthy conditions, where its levels are modulated by dietary intake of CLA and nitrite [17,19,22]. However, unlike human diets, both standard rodent chow and cell media are deficient in CLA thus making supplementation necessary for experimental purposes [36].

Using RAW264.7 cells and primary BMDM as models for resident and elicited macrophages, we show that NO$_2$-CLA formation occurs exclusively upon M1 polarization in an iNOS-dependent manner. Moreover, we demonstrate that macrophages are also capable of efficiently metabolizing NO$_2$-CLA via β-oxidation and nitroalkene reduction. Nitroalkene reduction by prostaglandin reductase-1 (PtGR-1) results in the formation of non-electrophilic nitroalkanes thus effectively inactivating their signaling actions [28]. This pathway, together with the intracellular formation of glutathione conjugates and dicarboxylic derivatives, are major contributors to the metabolic disposition of both endogenous and exogenously-administered NO$_2$-FA [22,37]. Interestingly, CLA nitration by LPS/IFN-γ-activated macrophages gives rise to the formation of two positional NO$_2$-CLA isomers in which $^\bullet$NO$_2$ adds to either C9 or C12. We find that 9-NO$_2$-CLA is metabolized less efficiently than 12-NO$_2$-CLA, suggesting that the proximity of the nitro group to the carboxylic end might decrease the metabolic rates of reduction of 9-NO$_2$-CLA by either PtGR-1 or other enzymatic processes involved in its β-oxidation (e.g. CoA thioester and carnitine ester formation, hydration, oxidation reactions). In contrast to these observations, experiments using synthetic 9- or 12-NO$_2$-CLA yielded no difference in terms of their ability to induce either HO-1 or NQO-1 expression. Similarly, both 9- and 12-NO$_2$-CLA dose-dependently inhibited LPS/IFN-γ induced iNOS expression with comparable potency. This supports that under acute treatment conditions such as those found in cell culture experiments, transcription factor engagement is an early event that takes place before cells are able to inactivate a quantitatively significant fraction of the added NO$_2$-CLA. However, over longer periods of time such as during inflammation-induced CLA nitration, 9-NO$_2$-CLA is likely to be the predominant species responsible for signaling reactions.
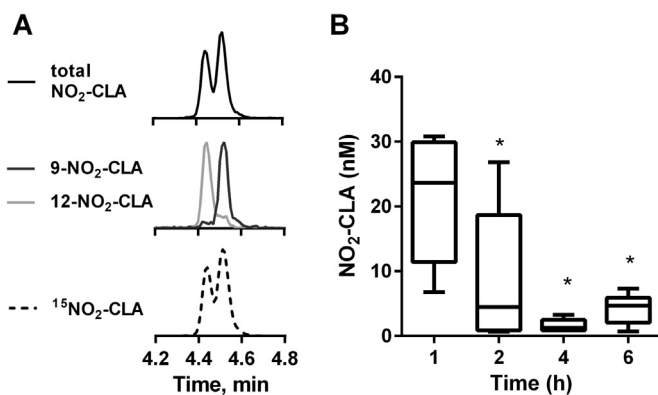
Fig. 6. Zymosan-A injection induces CLA nitration in vivo. A) Representative MRM traces showing total (MRM: 324/46, top); and specific 9- (324/168 dark grey, middle), 12-NO$_2$-CLA (324/157, light grey, middle) formation. Synthetic ^{15}N-labeled NO$_2$-CLA standard (bottom) showing chromatographic co-elution with the endogenous products in top and middle panels. B) Time course of peritoneal NO$_2$-CLA formation. Box and whiskers plot indicate median, 25th to 75th percentiles and range. * p < 0.05 versus 1 h time-point as determined by one-way ANOVA and Dunnett's multiple comparisons test (n = 6 per time point).

Fig. 7. NO₂-CLA modulates acute inflammatory responses *in vivo*. A) Representative flow cytometry dot plot of exudate cells from vehicle (PEG), CLA (2.5 mg/mouse) or NO₂-CLA (2.5 mg/kg). The dynamics of PMN infiltration are indicated in the gated population 12 h and 24 h post zymosan-A i.p. injection. B) Exudate PMN numbers were calculated. Results are mean ± SEM (n = 6 per time point). NO₂-CLA reduced PMN numbers as determined by two-way ANOVA and Holm-Sidak multiple comparisons test, * $p < 0.01$ and ** $p < 0.0001$ vs. PEG; # $p < 0.001$ and ## $p < 0.0001$ vs. CLA. C) Pro-inflammatory cytokines IL-6 and D) MCP-1 levels at 12 h. Results are mean ± SEM, (n = 6 per time point). * $p < 0.05$ as determined by one-way ANOVA.

The engagement of TLR proteins at the surface of myeloid, epithelial and endothelial cells by PAMPs or DAMPs, and the subsequent activation of NF-kB-dependent gene expression are key initiating events in the inflammatory response [7]. However, exaggerated or chronic activation of this pathway contributes to tissue injury and can lead to disease development [6,38,39]. In this regard, translation of Nrf2-dependent genes is crucial for cell survival in the presence of inflammation-derived oxygen and nitrogen reactive species [40]. As a result, the development of pharmacological agents capable of modulating TLR/NF-κB- and Nrf2-dependent pathways is a promising strategy for the treatment of

Scheme 1. Proposed model for NO₂-CLA formation and signaling actions under inflammatory conditions. Macrophage activation leads to iNOS expression, ˙NO-derived species formation and *in situ* NO₂-CLA generation. The electrophilic reactivity of the nitroalkene moiety in NO₂-CLA results in Nrf2 activation and in the inhibition of NF-κB dependent gene expression, thus inducing antioxidant/cytoprotective responses and limiting both reactive species generation and leukocyte recruitment to sites of inflammation. In addition to mediating CLA nitration, macrophages also regulate NO₂-CLA levels by β-oxidation and nitroalkene reduction to non-electrophilic nitroalkane derivatives.

dysregulated inflammation [40,41]. Herein, NO$_2$-CLA is shown to inhibit the expression of NF-κB-regulated genes and to activate ARE/Nrf2-dependent protein expression (Scheme 1). Interestingly, the inhibition of iNOS expression by NO$_2$-CLA suggested the presence of a negative feedback mechanism capable of down-regulating NO$_2$-FA formation, as iNOS-derived 'NO was shown to be required for CLA nitration. Moreover, whereas CLA was capable of dose-dependently inhibiting the transcription of NF-κB regulated genes, this phenomenon was abrogated when iNOS activity was absent. This demonstrates that the anti-inflammatory effects observed upon CLA addition to M1 polarized BMDMs are likely dependent on iNOS-induced NO$_2$-CLA formation. Our data clearly indicates that the role of macrophages in modulating NO$_2$-CLA levels extends beyond the generation of the precursor 'NO$_2$, as these cells also metabolize and inactivate NO$_2$-CLA. In this regard, these findings underscore the ability of the immune system to precisely titrate the generation of anti-inflammatory mediators and thus self-limit the severity of the inflammatory response.

In addition to changes in iNOS expression, the broad inhibitory actions of NO$_2$-CLA towards NF-κB-regulated gene expression also resulted in a reduction of pro-inflammatory cytokine release by activated macrophages. This observation was confirmed *in vivo* using an acute peritonitis model in which zymosan-A injection leads to cytokine-driven neutrophil and monocyte recruitment to the peritoneal cavity. In this model, administration of NO$_2$-CLA caused a significant reduction in PMN extravasation likely driven by a potent attenuation of IL-6 and MCP-1 levels. Notably, *in situ* CLA nitration was observed in this same peritonitis model, thus supporting the concept that NO$_2$-CLA formation may act as an endogenous regulator of inflammation *in vivo*.

CLA supplementation mediates protective immunomodulatory actions in animal models of rheumatoid arthritis [42,43], endotoxemia [44], asthma [45] and inflammatory bowel disease [46]. Although some of these benefits have been replicated in human trials [23,25], the overall clinical significance of these effects remains unclear [21,24]. Notably, the oral administration of CLA supplements in conjunction with either nitrite or nitrate, leads to increases in the systemic levels of NO$_2$-CLA in healthy human subjects [19]. Considering that the diet is also an important source of nitrite/nitrate intake [20] and that the gastric compartment is a prominent site for CLA nitration [17], it is tempting to speculate that at least part of the variability observed within and across CLA human trials might be related to lack of nitrite/nitrate intake control among participants. In this regard, it has been proposed that the intra-gastric formation of NO$_2$-FA is a central contributor to the cardiovascular benefits ascribed to the Mediterranean diet [47]. Finally, lactic acid bacteria in the gut microbiota have been shown to isomerize bis-allylic linoleic acid as well as α- and γ-linolenic acid to generate CLA, thus adding another layer of complexity to the understanding of the physiological effects of this fatty acid [48].

The therapeutic potential of exogenously-administered NO$_2$-FA has been extensively studied [47,49–52]. However, the question of whether NO$_2$-FA endogenously function as adaptive signaling mediators under physiological conditions still poses a challenge. *In vitro*, concentrations above 1 μM are required for NO$_2$-CLA to exert its signaling actions, while the highest level detected in peritoneal lavage is ~30 nM. Importantly, although the concentration of NO$_2$-CLA in the native peritoneal fluid is likely to be 5–20 fold greater than that measured in more diluted 1 mL lavage fractions, comparing effective concentrations obtained from cell culture experiments to those detected in an *in vivo* setting can be misleading. Unlike *in vitro* studies, when NO$_2$-CLA is added as a bolus, measurement of *in vivo* concentrations reflect the contribution of individual rates of formation, degradation, esterification in complex lipids [53], thiol addition and whole body distribution at a given point in time. In addition, our ability to detect peritoneal NO$_2$-CLA is also limited by the efficiency of the PBS lavage in recovering a chemically-reactive fatty acid derivative from the peritoneal cavity. Thus, while nanomolar NO$_2$-CLA concentrations are detected in the peritoneal lavage, the actual cellular exposure can be significantly

greater. Also, contrary to saturation kinetics, where concentration is critical for defining ligand binding and biological action, electrophilic compounds are characterized by low dissociation constants and high target residency times [13,54,55]. This implies that the stimulation of local NO$_2$-CLA formation will sustain signaling responses long after significant fractions of the initially formed compound have been removed by metabolic, diffusion and transport processes. Our results demonstrate that by mediating CLA nitration, the immune system is capable of generating an electrophilic NO$_2$-FA with the potential to influence the progression of the inflammatory response. As a result, NO$_2$-CLA generation during inflammatory processes represents an autocrine response that is limited to the immediate vicinity of the site of lipid electrophile formation In this regard, NO$_2$-CLA biology somewhat resembles that of mediators such as hydroxylated ω3-fatty acid derivatives (resolvins, lipoxins, protectins and maresins) as these compounds share anti-inflammatory properties and are also detected at relatively low concentrations [56]. Nonetheless, several differences become apparent as the latter species are enzymatically generated, exert signaling actions through ligation of G-protein coupled receptors and lack electrophilic reactivity. In this regard, the mechanisms of formation and action of NO$_2$-CLA are more closely related to those exhibited by other ω − 3 and arachidonic acid-derived electrophiles [57,58].

Herein, we show that activated leukocytes mediate CLA nitration resulting in NO$_2$-CLA formation *in vitro* and *in vivo*. In addition, NO$_2$-CLA administration to activated macrophages and zymosan-A treated mice inhibits NF-κB-regulated gene expression, decreases pro-inflammatory cytokine production, attenuates PMN recruitment to the peritoneum and promotes the expression of Nrf2-dependent cytoprotective and antioxidant proteins. Taken together, our results support that iNOS-dependent generation of NO$_2$-CLA is an adaptive signaling mechanism that allows the immune system to fine-tune the magnitude of the inflammatory response while simultaneously protecting neighboring tissues from the damaging effects of reactive oxygen and nitrogen species.

4. Experimental procedures

4.1. Materials

Reagents were of analytical grade or higher and were purchased from Sigma (St. Louis, MO, USA) unless otherwise stated. (9*Z*,11*E*)-octadecadienoic acid (CLA, 90%) was obtained from Nu-Check Prep, Inc (Elysian, MN, USA), 9- and 12-nitro-octadeca-9,11-dienoic acid (9-NO$_2$-CLA and 12-NO$_2$-CLA) were synthesized as described previously [59,60], The term NO$_2$-CLA refers to a mixture of the aforementioned positional isomers. ^{15}N-labeled dihydro-9-NO$_2$-CLA (11,12-dihydro-9-NO$_2$-CLA) was generated by incubating 9-^{15}NO$_2$-CLA with purified rat PtGR-1 [28]. The concentration of all NO$_2$-CLA stocks was measured prior to each experiment using the same extinction coefficient of 11.2 mM^{-1}cm^{-1} at 312 nm in methanol for both 9- and 12-NO$_2$ positional isomers.

4.2. Animals

Male C57BL/6 J and iNOS knockout mice (Stock No: 002609) (12 weeks old) were obtained from the Jackson Laboratories. All mice were maintained in a temperature- and light-controlled environment and were fed standard diet (PicoLab rodent diet 5LOD; LabDiet) and water ad libitum. Animal experiments were approved by the Institutional Animal Care & Use Committee on Animals of the University of Michigan (PRO00006176) and the University of Pittsburgh (14084265) and performed in accordance with institutional guidelines.

4.3. Cell culture

RAW264.7 cells were obtained from ATCC (Manassas, VA, USA) and maintained in DMEM (Mediatech, Manassas, VA, USA) supplemented with fetal bovine serum (FBS, 10%, Gibco-Life Technologies, Waltham, MA, USA) at 37 °C, 5% CO_2 and 95% humidity. Cell activation was induced by treatment with 100 ng/mL LPS plus 200 U/mL recombinant mouse IFN-γ (BD Biosciences, San Jose, CA, USA) in the presence of varying concentrations of CLA and 1% FBS. BMDM were obtained from bone marrow cells from C57BL/6 J and iNOS knockout mice by flushing the marrow from femurs with RPMI containing 10% FBS. The marrow plugs were disrupted into a single cell suspension, cultured in RPMI containing 10% FBS supplemented with 15% L-929 cell-conditioned medium at a density of 1×10^6 cells. After 7 days, adherent BMDM cells were washed with PBS and medium replaced with RPMI, 1% FBS, 15% L-929 cell-conditioned medium overnight (M0). Cells were then differentiated into M1 (LPS 100 ng/mL + IFN-γ (200 U/mL), or M2 (IL-4 20 ng/mL) macrophages in the presence of varying concentrations of CLA or NO_2-CLA for the indicated periods. Cell media was collected at the indicated times and nitrated lipids were obtained as described below. For metabolite electrophilicity assessment, cell media was incubated with 500 mM BME for 2 h at 37 °C prior to lipid extraction. For western blot analysis, cells were lysed in CellLytic M (Sigma) following manufacturer's instructions, proteins resolved by SDS-PAGE and transferred onto nitrocellulose membranes. The following antibodies were used: iNOS (BD #610333, 1:1000), HO-1 (Cell Signaling #5061 S, 1:1000), NQO1 (Abcam #ab341732, 1:000), GAPDH (Trevigen #2275, 1:5000), Actin (Sigma #A4700, 1:3000). Blocking and antibody incubations were performed using 1% Casein/PBS solution (Bio-rad, Hercules, CA). Secondary HRP-conjugated antibodies were from Cell Signaling and were used at a 1:2000 dilution.

4.4. Preparation of L-929 cell conditioned medium

Mouse L-929 conditioned medium was used as a source of colony-stimulating factor activity. The L-929 cells were grown in RPMI supplemented with 10% FCS with fresh medium added every 3 days (20% v/v). After 10 days, the culture medium was removed, and filtered (0.22 pm filter) and used for BMDM culture.

4.5. Total RNA reparation and RT-qPCR analysis

Total RNA was isolated from the cells using RNeasy Kit (Qiagen). RNA was reverse-transcribed into cDNA with SuperScript III (Invitrogen) using random primers. The expression of target genes was determined by a qPCR System (Bio-Rad) using iQ SYBR Green Supermix (Bio-Rad). Gene expression was normalized against the expression of the internal control, 18 S. Primer sequences are detailed in Table S1.

4.6. Cytokine measurements

For cell-based studies, 1×10^4 RAW 264.7 cells were plated in 96 well plates and cultured until confluent. Cells were then treated for 24 h with 100 ng/mL LPS in the presence or absence of NO_2-CLA and media was collected for analysis. In the case of peritoneal cytokines, the peritoneum cavity was lavaged 12 h after zymosan-A injection (1 mg/mouse) in the presence or absence of NO_2-CLA co-treatment (2.5 mg/kg) using 1 mL phosphate-buffered saline. IL-6 (BD #555240) and MCP-1 (BD #555260) were measured in media and lavageates by ELISA following manufacturer's instructions.

4.7. Reporter assays

Firefly luciferase-based reporter cell lines were obtained from BPS Bioscience (San Diego, CA, USA) and were cultured according to manufacturer instructions with the exception that cells were grown in

20% FBS medium immediately after thawing. The Nrf2/ARE reporter (catalog number 60513) contains a firefly luciferase gene under the control of ARE (antioxidant response element) which is stably integrated into HepG2 cells. ARE reporter (Luc)-HepG2 cells were treated with the indicated concentrations of NO_2-CLA isomers or vehicle for 18 h in complete medium (10% FBS supplemented with 600 μg/mL Geneticin). NF-κB reporter (Luc)-HEK293 (catalog number 60650) contains the firefly luciferase gene under 4 tandem copy repeats of the NF-κB response element (located upstream of minimal TATA promoter) stably integrated into cells. These cells were activated with 500 pg/mL TNF-α in the presence or absence of NO_2-CLA in full medium (10% FBS plus 50 μg/mL Hygromycin B) for 2 h. Luciferase activity was assessed using a Luciferase Assay System from Promega (Madison, WI, USA).

4.8. Zymosan-A induced peritonitis

Mice were injected with zymosan-A (1 mg/mouse, i.p.) and either NO_2-CLA (2.5 mg/kg), CLA (2.5 mg/mouse), dissolved in poly-ethylene-glycol (PEG) plus PBS (1:1). Peritoneal exudates (1 mL, phosphate-buffered saline) were collected at the indicated time intervals (0, 12, 24 h) and processed for flow cytometry analysis.

4.9. Flow cytometry

Leukocyte numbers and differential counts were performed using a Luna Automated Cell Counter (Logos Biosystems) and flow cytometry analysis. Peritoneal exudate cells were incubated with anti-mouse CD16/32 antibody (clone 2.4G2, Tonbo Bioscience, San Diego, CA, USA) (0.5 μg per 10^6 cells) for 5 min to block FcγRII/III receptors and then incubated (30 min, 4 °C) with PE anti CD11b antibody (clone: M1/70, Tonbo Bioscience), PE-Cy7 anti Ly-6C antibody (clone: AL-21, BD Biosciences, San Jose, CA, USA), APC anti F4/80 antibody (clone BM8.1, BD Biosciences) and PerCP-Cy5.5 anti Ly-6G antibody (clone: 1A8, BD Biosciences) to determine leukocyte sub-types. After washing, cells were incubated with 2.5 μg/mL DAPI to exclude dead or dying cells (DAPI-negative). Fluorescence minus one (FMO) controls were used for gating analyses. Compensation was performed using single color controls prepared from UltraComp eBeads (eBioscience, San Diego, CA, USA). Gating strategy including live/death cell discrimination, sizing and upper threshold analysis using FMO is depicted in Suppl Fig. 2. Flow cytometric data were collected on a Cyan 5 flow cytometer (Beckman Coulter) located at the University of Michigan Flow Cytometry Core Facility and analyzed with FloJo software (Tree Star).

4.10. Lipid extraction

RAW264.7 culture media and cell-free peritoneal exudates were spiked with 10 μL of a 1 μM solution of internal standard, treated with 20 mM mercury (II) chloride ($HgCl_2$) for 30 min at 37 °C followed by C18 solid phase extraction (Sep-Pak, Waters, Milford, MA, USA) as described [22]. Briefly, columns were activated with methanol, equilibrated and samples were loaded in 10% methanol/water. Columns were then washed (10% methanol), dried under vacuum, and lipids eluted using 100% methanol. Cell media from BMDM was treated with $HgCl_2$ and internal standard as before followed by supplementation with 1% (w/v) sulfanilamide. Lipids were extracted with 1 mL 1 M formic acid: isopropanol:hexanes (2:20:30, vol/vol/vol) followed by an additional 1 mL of hexanes. Organic extracts and C18 eluates were dried under nitrogen, resuspended in methanol and subjected to LC-MS/MS analysis.

4.11. LC-MS/MS determinations

Nitrated fatty acids were resolved by reverse-phase chromatography (C18 Luna column: 2×100 mm, 5 μm particle size; Phenomenex) at a 0.65 mL/min flow rate using acetonitrile/water supplemented with

0.1% acetic acid as the mobile phase. Cell media extracts were injected at 20% acetonitrile/acetic acid for 0.3 min, followed by a linear increase in the organic phase to 100% over 10 min. The mobile phase composition was kept constant for 3 min and then the column was re-equilibrated at 20% for 3 min. Peritoneal lavage samples were loaded at 35% acetonitrile/acetic acid for 0.3 min, followed by a linear increase in the organic phase to 100% over 4.7 min. The column was washed at 100% for 2 min and then re-equilibrated at 35% for 3 min. The analysis was performed using either an API 5000 or a Q-Trap 6500+ mass spectrometer (Applied Biosystems, Framingham, MA) in the negative ion mode. Source temperature was 600 °C, curtain gas: 40, ionization spray voltage: −4500, GS1: 55, GS2: 60. For collision induced fragmentations leading to either $^{14}NO_2^-$ or $^{15}NO_2^-$ formation (m/z 46 and 47 respectively), the following settings were used: declustering potential: −80 V, entrance potential: −5 V, collision energy: −35 V and collision cell exit potential: −3 V. The corresponding MRM transitions are: NO_2-CLA (324.2/46), dihydro-NO_2-CLA (326/46), $^{13}C_{18}$ NO_2-OA (344.2/46), $^{15}NO_2$-CLA (325.2/47), and $d_4^{15}N$-NO_2-OA (331.2/47). Transitions for β-oxidation metabolites were obtained by subtracting 28 amu from parent compounds and following collision induced generation of 46 m/z ions as before [22]. For 9-NO_2-CLA (324.2/168, 324.2/210) and 12-NO_2-CLA (324.2/157, 324.2/171.2) MRM analysis, the collision energy was set to -20V. High resolution determinations were performed in collision-induced dissociation (CID) mode using an LTQ Velos Orbitrap (Thermo Scientific, Waltham, MA, USA) equipped with a HESI II electrospray source. The following parameters were used: source temperature 450 °C, capillary temperature 360 °C, sheath gas flow 20, auxiliary gas flow 15, sweep gas flow 3, Ion spray voltage 4 kV, S-lens RF level 41 (%). The instrument FT-mode was calibrated using the manufacturer's recommended calibration solution with the addition of malic acid as a low m/z calibration point in the negative ion mode. The quantification of NO_2-CLA isomers and the corresponding dihydro metabolites was performed by isotopic dilution using calibration curves constructed with synthetic NO_2-CLA in the presence of either $^{13}C_{18}$ NO_2-OA or $d_4^{15}N$-NO_2-OA as internal standards.

Acknowledgments

Declaration of interest

FJS, NKK, SRW, BAF and DAV acknowledge financial interest in Complexa, Inc.

Author contributions

LV contributed to the overall concept, designed, performed and analyzed all *in vivo* experiments and participated in manuscript preparation. LM performed experiments and analyzed the data. SRS developed LC-MS/MS methodology and performed high resolution MS/MS experiments. NKK designed and analyzed reporter assay experiments. OR, ZG and RCB performed *in vivo* experiments and BMDM isolations. SJ performed protein expression experiments. LL performed cell-based reporter assays. SRW synthesized mixed and pure positional NO_2-CLA isomers. YEC and BAF contributed to concept development and manuscript preparation. AMF analyzed flow cytometry data and contributed to experimental and manuscript design. FJS designed and interpreted experiments, contributed to the overall concept and assisted with manuscript preparation. DAV designed, coordinated and performed experiments, analyzed data and wrote the manuscript.

Appendix A. Supporting information

Supplementary data associated with this article can be found in the online version at http://dx.doi.org/10.1016/j.redox.2018.01.005.

References

[1] M.A. Sugimoto, L.P. Sousa, V. Pinho, M. Perretti, M.M. Teixeira, Resolution of inflammation: what controls its onset? Front. Immunol. 7 (2016) 160, http://dx.doi.org/10.3389/fimmu.2016.00160.

[2] M.F. Gregor, G.S. Hotamisligil, Inflammatory mechanisms in obesity, Rev. Immunol. 29 (2011) 415–445, http://dx.doi.org/10.1146/annurev-immunol-031210-101322.

[3] M.G. Sorci-Thomas, M.J. Thomas, Microdomains, inflammation, and atherosclerosis, Circ. Res. 118 (2016) 679–691, http://dx.doi.org/10.1161/CIRCRESAHA.115.306246.

[4] C. Emerging Risk Factors, S. Kaptoge, E. Di Angelantonio, G. Lowe, M.B. Pepys, S.G. Thompson, R. Collins, J. Danesh, C-reactive protein concentration and risk of coronary heart disease, stroke, and mortality: an individual participant meta-analysis, Lancet 375 (2010) 132–140, http://dx.doi.org/10.1016/S0140-6736(09)61717-7.

[5] C.C. Esenwa, M.S. Elkind, Inflammatory risk factors, biomarkers and associated therapy in ischaemic stroke, Nat. Rev. Neurol. 12 (2016) 594–604, http://dx.doi.org/10.1038/nrneurol.2016.125.

[6] N. Glezeva, S. Horgan, J.A. Baugh, Monocyte and macrophage subsets along the continuum to heart failure: misguided heroes or targetable villains? J. Mol. Cell Cardiol. 89 (2015) 136–145, http://dx.doi.org/10.1016/j.yjmcc.2015.10.029.

[7] C.A. Leifer, A.E. Medvedev, Molecular mechanisms of regulation of Toll-like receptor signaling, J. Leukoc. Biol. 100 (2016) 927–941, http://dx.doi.org/10.1189/jlb.2MR0316-117RR.

[8] P. Pacher, J.S. Beckman, L. Liaudet, Nitric oxide and peroxynitrite in health and disease, Physiol. Rev. 87 (2007) 315–424, http://dx.doi.org/10.1152/physrev.00029.2006.

[9] S. Baldus, J.P. Eiserich, M.L. Brennan, R.M. Jackson, C.B. Alexander, B.A. Freeman, Spatial mapping of pulmonary and vascular nitrotyrosine reveals the pivotal role of myeloperoxidase as a catalyst for tyrosine nitration in inflammatory diseases, Free Radic. Biol. Med. 33 (2002) 1010, http://dx.doi.org/10.1016/S0891-5849(02)00993-0.

[10] N.V. Serbina, T. Jia, T.M. Hohl, E.G. Pamer, Monocyte-mediated defense against microbial pathogens, Annu. Rev. Immunol. 26 (2008) 421–452, http://dx.doi.org/10.1146/annurev.immunol.26.021607.090326.

[11] W.A. Pryor, J.W. Lightsey, D.F. Church, Reaction of nitrogen dioxide with alkenes and polyunsaturated fatty acids: addition and hydrogen-abstraction mechanisms, J. Am. Chem. Soc. 104 (1982) 6685–6692, http://dx.doi.org/10.1021/ja00388a035.

[12] C. Batthyany, F.J. Schopfer, P.R. Baker, R. Duran, L.M. Baker, Y. Huang, C. Cervenansky, B.P. Branchaud, B.A. Freeman, Reversible post-translational modification of proteins by nitrated fatty acids in vivo, J. Biol. Chem. 281 (2006) 20450–20463, http://dx.doi.org/10.1074/jbc.M602814200.

[13] L. Turell, D.A. Vitturi, E.L. Coitino, L. Lebrato, M.N. Moller, C. Sagasti, S.R. Salvatore, S.R. Woodcock, B. Alvarez, F.J. Schopfer, The chemical basis of thiol addition to nitro-conjugated linoleic acid, a protective cell-signaling lipid, J. Biol. Chem. 292 (2017) 1145–1159, http://dx.doi.org/10.1074/jbc.M116.756288.

[14] M. Delmastro-Greenwood, B.A. Freeman, S.G. Wendell, Redox-dependent anti-inflammatory signaling actions of unsaturated fatty acids, Annu. Rev. Physiol. 76 (2014) 79–105, http://dx.doi.org/10.1146/annurev-physiol-021113-170341.

[15] T. Ichikawa, J. Zhang, K. Chen, Y. Liu, F.J. Schopfer, P.R. Baker, B.A. Freeman, Y.E. Chen, T. Cui, Nitroalkenes suppress lipopolysaccharide-induced signal transducer and activator of transcription signaling in macrophages: a critical role of mitogen-activated protein kinase phosphatase 1, Endocrinology 149 (2008) 4086–4094, http://dx.doi.org/10.1210/en.2007-1639.

[16] L. Villacorta, Z. Gao, F.J. Schopfer, B.A. Freeman, Y.E. Chen, Nitro-fatty acids in cardiovascular regulation and diseases: characteristics and molecular mechanisms, Front Biosci. (Landmark Ed) 21 (2016) 873–889, http://dx.doi.org/10.2741/4425.

[17] G. Bonacci, P.R. Baker, S.R. Salvatore, D. Shores, N.K. Khoo, J.R. Koenitzer, D.A. Vitturi, S.R. Woodcock, F. Golin-Bisello, M.P. Cole, et al., Conjugated linoleic acid is a preferential substrate for fatty acid nitration, J. Biol. Chem. 287 (2012) 44071–44082, http://dx.doi.org/10.1074/jbc.M112.401356.

[18] H.H. Bjorne, J. Petersson, M. Phillipson, E. Weitzberg, L. Holm, J.O. Lundberg, Nitrite in saliva increases gastric mucosal blood flow and mucus thickness, J. Clin. Investig. 113 (2004) 106–114, http://dx.doi.org/10.1172/JCI19019.

[19] M. Delmastro-Greenwood, K.S. Hughan, D.A. Vitturi, S.R. Salvatore, G. Grimes, G. Potti, S. Shiva, F.J. Schopfer, M.T. Gladwin, B.A. Freeman, et al., Nitrite and nitrate-dependent generation of anti-inflammatory fatty acid nitroalkenes, Free Radic. Biol. Med. 89 (2015) 333–341, http://dx.doi.org/10.1016/j.freeradbiomed.2015.07.149.

[20] N.G. Hord, Y. Tang, N.S. Bryan, Food sources of nitrates and nitrites: the physiologic context for potential health benefits, Am. J. Clin. Nutr. 90 (2009) 1–10, http://dx.doi.org/10.3945/ajcn.2008.27131.

[21] J.H. Kim, Y. Kim, Y.J. Kim, Y. Park, Conjugated linoleic acid: potential health benefits as a functional food ingredient, Annu. Rev. Food Sci. Technol. 7 (2016) 221–244, http://dx.doi.org/10.1146/annurev-food-041715-033028.

[22] S.R. Salvatore, D.A. Vitturi, P.R. Baker, G. Bonacci, J.R. Koenitzer, S.R. Woodcock, B.A. Freeman, F.J. Schopfer, Characterization and quantification of endogenous fatty acid nitroalkene metabolites in human urine, J. Lipid Res. 54 (2013)

1998–2009, http://dx.doi.org/10.1194/jlr.M037804.

[23] N. Aryaeian, M. Djalali, F. Shahram, A. Djazayery, M.R. Eshragian, Effect of conjugated linoleic Acid, vitamin e, alone or combined on immunity and inflammatory parameters in adults with active rheumatoid arthritis: a randomized controlled trial, Int. J. Prev. Med. 5 (2014) 1567–1577.

[24] A. Bhattacharya, J. Banu, M. Rahman, J. Causey, G. Fernandes, Biological effects of conjugated linoleic acids in health and disease, J. Nutr. Biochem 17 (2006) 789–810, http://dx.doi.org/10.1016/j.jnutbio.2006.02.009.

[25] L.A. Penedo, J.C. Nunes, M.A. Gama, P.E. Leite, T.F. Quirico-Santos, A.G. Torres, Intake of butter naturally enriched withcis9, trans11 conjugated linoleic acid reduces systemic inflammatory mediators in healthy young adults, J. Nutr. Biochem. 24 (2013) 2144–2151, http://dx.doi.org/10.1016/j.jnutbio.2013.08.006.

[26] G. Bonacci, E.K. Asciutto, S.R. Woodcock, S.R. Salvatore, B.A. Freeman, F.J. Schopfer, Gas-phase fragmentation analysis of nitro-fatty acids, J. Am. Soc. Mass Spectrom. 22 (2011) 1534–1551, http://dx.doi.org/10.1007/s13361-011-0185-x.

[27] V. Rudolph, F.J. Schopfer, N.K. Khoo, T.K. Rudolph, M.P. Cole, S.R. Woodcock, G. Bonacci, A.L. Groeger, F. Golin-Bisello, C.S. Chen, et al., Nitro-fatty acid metabolome: saturation, desaturation, beta-oxidation, and protein adduction, J. Biol. Chem. 284 (2009) 1461–1473, http://dx.doi.org/10.1074/jbc.M802298200.

[28] D.A. Vitturi, C.S. Chen, S.R. Woodcock, S.R. Salvatore, G. Bonacci, J.R. Koenitzer, N.A. Stewart, N. Wakabayashi, T.W. Kensler, B.A. Freeman, et al., Modulation of nitro-fatty acid signaling: prostaglandin reductase-1 is a nitroalkene reductase, J. Biol. Chem. 288 (2013) 25626–25637, http://dx.doi.org/10.1074/jbc.M113.486282.

[29] R.P. Claridge, A.J. Deeming, N. Paul, D.A. Tocher, J.H. Ridd, The reactions of nitrogen dioxide with dienes, J. Chem. Soc., Perkin Trans. 1 (1998) 3523–3528, http://dx.doi.org/10.1039/a806451b.

[30] E. Kansanen, G. Bonacci, F.J. Schopfer, S.M. Kuosmanen, K.I. Tong, H. Leinonen, S.R. Woodcock, M. Yamamoto, C. Carlberg, S. Yla-Herttuala, et al., Electrophilic nitro-fatty acids activate NRF2 by a KEAP1 cysteine 151-independent mechanism, J. Biol. Chem. 286 (2011) 14019–14027, http://dx.doi.org/10.1074/jbc.M110.190710.

[31] K. Takaya, T. Suzuki, H. Motohashi, K. Onodera, S. Satomi, T.W. Kensler, M. Yamamoto, Validation of the multiple sensor mechanism of the Keap1-Nrf2 system, Free Radic. Biol. Med. 53 (2012) 817–827, http://dx.doi.org/10.1016/j.freeradbiomed.2012.06.023.

[32] L. Villacorta, J. Zhang, M.T. Garcia-Barrio, X.L. Chen, B.A. Freeman, Y.E. Chen, T. Cui, Nitro-linoleic acid inhibits vascular smooth muscle cell proliferation via the Keap1/Nrf2 signaling pathway, Am. J. Physiol. Heart Circ. Physiol. 293 (2007) H770–H776, http://dx.doi.org/10.1152/ajpheart.00261.2007.

[33] M.M. Wright, J. Kim, T.D. Hock, N. Leitinger, B.A. Freeman, A. Agarwal, Human haem oxygenase-1 induction by nitro-linoleic acid is mediated by cAMP, AP-1 and E-box response element interactions, Biochem. J. 422 (2009) 353–361, http://dx.doi.org/10.1042/BJ20090339.

[34] G.L. Bannenberg, N. Chiang, A. Ariel, M. Arita, E. Tjonahen, K.H. Gotlinger, S. Hong, C.N. Serhan, Molecular circuits of resolution: formation and actions of resolvins and protectins, J. Immunol. 174 (2005) 4345–4355, http://dx.doi.org/10.4049/jimmunol.174.7.4345.

[35] D.A. Vitturi, L. Minarrieta, S.R. Salvatore, E.M. Postlethwait, M. Fazzari, G. Ferrer-Sueta, J.R. Lancaster Jr., B.A. Freeman, F.J. Schopfer, Convergence of biological nitration and nitrosation via symmetrical nitrous anhydride, Nat. Chem. Biol. 11 (2015) 504–510, http://dx.doi.org/10.1038/nchembio.1814.

[36] Y.W. Wang, P.J. Jones, Conjugated linoleic acid and obesity control: efficacy and mechanisms, Int. J. Obes. Relat. Metab. Disord. 28 (2004) 941–955, http://dx.doi.org/10.1038/sj.ijo.0802641.

[37] S.R. Salvatore, D.A. Vitturi, M. Fazzari, D.K. Jorkasky, F.J. Schopfer, Evaluation of 10-nitro oleic acid bio-elimination in rats and humans, Sci. Rep. 7 (2017) 39900, http://dx.doi.org/10.1038/srep39900.

[38] M.J. Delano, P.A. Ward, The immune system's role in sepsis progression, resolution, and long-term outcome, Immunol. Rev. 274 (2016) 330–353, http://dx.doi.org/10.1111/imr.12499.

[39] D. Zhang, C. Xu, D. Manwani, P.S. Frenette, Neutrophils, platelets, and inflammatory pathways at the nexus of sickle cell disease pathophysiology, Blood 127 (2016) 801–809, http://dx.doi.org/10.1182/blood-2015-09-618538.

[40] T. Suzuki, H. Motohashi, M. Yamamoto, Toward clinical application of the Keap1-Nrf2 pathway, Trends Pharmacol. Sci. 34 (2013) 340–346, http://dx.doi.org/10.1016/j.tips.2013.04.005.

[41] S.K. Arepalli, M. Choi, J.K. Jung, H. Lee, Novel NF-kappaB inhibitors: a patent review (2011–2014), Expert Opin. Ther. Pat. 25 (2015) 319–334, http://dx.doi.org/10.1517/13543776.2014.998199.

[42] D.E. Butz, G. Li, S.M. Huebner, M.E. Cook, A mechanistic approach to understanding conjugated linoleic acid's role in inflammation using murine models of rheumatoid arthritis, Am. J. Physiol. Regul. Integr. Comp. Physiol. 293 (2007) R669–R676, http://dx.doi.org/10.1152/ajpregu.00005.2007.

[43] S.M. Huebner, J.M. Olson, J.P. Campbell, J.W. Bishop, P.M. Crump, M.E. Cook, Low dietary c9t11-conjugated linoleic acid intake from dairy fat or supplements reduces inflammation in collagen-induced arthritis, Lipids 51 (2016) 807–819, http://dx.doi.org/10.1007/s11745-016-4163-8.

[44] C.M. Reynolds, E. Draper, B. Keogh, A. Rahman, A.P. Moloney, K.H. Mills, C.E. Loscher, H.M. Roche, A conjugated linoleic acid-enriched beef diet attenuates lipopolysaccharide-induced inflammation in mice in part through PPARgamma-mediated suppression of toll-like receptor 4, J. Nutr. 139 (2009) 2351–2357, http://dx.doi.org/10.3945/jn.109.113035.

[45] A. Jaudszus, M. Krokowski, P. Mockel, Y. Darcan, A. Avagyan, P. Matricardi, G. Jahreis, E. Hamelmann, Cis-9,trans-11-conjugated linoleic acid inhibits allergic sensitization and airway inflammation via a PPARgamma-related mechanism in mice, J. Nutr. 138 (2008) 1336–1342.

[46] J. Bassaganya-Riera, K. Reynolds, S. Martino-Catt, Y. Cui, L. Hennighausen, F. Gonzalez, J. Rohrer, A.U. Benninghoff, R. Hontecillas, Activation of PPAR gamma and delta by conjugated linoleic acid mediates protection from experimental inflammatory bowel disease, Gastroenterology 127 (2004) 777–791, http://dx.doi.org/10.1053/j.gastro.2004.06.049.

[47] R.L. Charles, O. Rudyk, O. Prysyazhna, A. Kamynina, J. Yang, C. Morisseau, B.D. Hammock, B.A. Freeman, P. Eaton, Protection from hypertension in mice by the Mediterranean diet is mediated by nitro fatty acid inhibition of soluble epoxide hydrolase, Proc. Natl. Acad. Sci. USA 111 (2014) 8167–8172, http://dx.doi.org/10.1073/pnas.1402965111.

[48] S. Kishino, M. Takeuchi, S.B. Park, A. Hirata, N. Kitamura, J. Kunisawa, H. Kiyono, R. Iwamoto, Y. Isobe, M. Arita, et al., Polyunsaturated fatty acid saturation by gut lactic acid bacteria affecting host lipid composition, Proc. Natl. Acad. Sci. USA 110 (2013) 17808–17813, http://dx.doi.org/10.1073/pnas.1312937110.

[49] E.E. Kelley, J. Baust, G. Bonacci, F. Golin-Bisello, J.E. Devlin, C.M. St Croix, S.C. Watkins, S. Gor, N. Cantu-Medellin, E.R. Weidert, et al., Fatty acid nitroalkenes ameliorate glucose intolerance and pulmonary hypertension in high-fat diet-induced obesity, Cardiovasc Res 101 (2014) 352–363, http://dx.doi.org/10.1093/cvr/cvt341.

[50] A. Klinke, A. Moller, M. Pekarova, T. Ravekes, K. Friedrichs, M. Berlin, K.M. Scheu, L. Kubala, G. Ambrozova, et al., Protective effects of 10-nitro-oleic acid in a hypoxia-induced murine model of pulmonary hypertension, Am. J. Respir. Cell Mol. Biol. 51 (2014) 155–162, http://dx.doi.org/10.1165/rcmb.2013-0063OC.

[51] T.K. Rudolph, V. Rudolph, M.M. Edreira, M.P. Cole, G. Bonacci, F.J. Schopfer, S.R. Woodcock, A. Franek, M. Pekarova, N.K. Khoo, et al., Nitro-fatty acids reduce atherosclerosis in apolipoprotein E-deficient mice, Arterioscler. Thromb. Vasc. Biol. 30 (2010) 938–945, http://dx.doi.org/10.1161/ATVBAHA.109.201582.

[52] L. Villacorta, L. Chang, S.R. Salvatore, T. Ichikawa, J. Zhang, D. Petrovic-Djergovic, L. Jia, H. Carlsen, F.J. Schopfer, B.A. Freeman, et al., Electrophilic nitro-fatty acids inhibit vascular inflammation by disrupting LPS-dependent TLR4 signalling in lipid rafts, Cardiovasc Res. 98 (2013) 116–124, http://dx.doi.org/10.1093/cvr/cvt002.

[53] M. Fazzari, N.K. Khoo, S.R. Woodcock, D.K. Jorkasky, L. Li, F.J. Schopfer, B.A. Freeman, Nitro-fatty acid pharmacokinetics in the adipose tissue compartment, J. Lipid Res. 58 (2017) 375–385, http://dx.doi.org/10.1194/jlr.M072058.

[54] R.A. Copeland, D.L. Pompliano, T.D. Meek, Drug-target residence time and its implications for lead optimization, Nat. Rev. Drug Discov. 5 (2006) 730–739, http://dx.doi.org/10.1038/nrd2082.

[55] J.Y. Oh, N. Giles, A. Landar, V. Darley-Usmar, Accumulation of 15-deoxy-delta (12,14)-prostaglandin J2 adduct formation with Keap1 over time: effects on potency for intracellular antioxidant defence induction, Biochem. J. 411 (2008) 297–306, http://dx.doi.org/10.1042/bj20071189.

[56] C.N. Serhan, N. Chiang, J. Dalli, New pro-resolving n-3 mediators bridge resolution of infectious inflammation to tissue regeneration, Mol. Asp. Med. (2017), http://dx.doi.org/10.1016/j.mam.2017.08.002.

[57] A.L. Groeger, C. Cipollina, M.P. Cole, S.R. Woodcock, G. Bonacci, T.K. Rudolph, V. Rudolph, B.A. Freeman, F.J. Schopfer, Cyclooxygenase-2 generates anti-inflammatory mediators from omega-3 fatty acids, Nat. Chem. Biol. 6 (2010) 433–441, http://dx.doi.org/10.1038/nchembio.367.

[58] K. Uchida, T. Shibata, 15-deoxy-delta(12,14)-prostaglandin J2: an electrophilic trigger of cellular responses, Chem. Res. Toxicol. 21 (2008) 138–144, http://dx.doi.org/10.1021/tx700177j.

[59] S.R. Woodcock, G. Bonacci, S.L. Gelhaus, F.J. Schopfer, Nitrated fatty acids: synthesis and measurement, Free Radic. Biol. Med. 59 (2013) 14–26, http://dx.doi.org/10.1016/j.freeradbiomed.2012.11.015.

[60] S.R. Woodcock, S.R. Salvatore, G. Bonacci, F.J. Schopfer, B.A. Freeman, Biomimetic nitration of conjugated linoleic acid: formation and characterization of naturally occurring conjugated nitrodienes, J. Org. Chem. 79 (2014) 25–33, http://dx.doi.org/10.1021/jo4021562.